

SOLPS-ITER numerical evaluation about the effect of drifts in a divertor configuration of ASDEX-Upgrade and a limiter configuration of J-TEXT

Original

SOLPS-ITER numerical evaluation about the effect of drifts in a divertor configuration of ASDEX-Upgrade and a limiter configuration of J-TEXT / Wu, H., Shi, P., Subba, F., Sun, H., Wischmeier, M., Zanino, R.. - In: FUSION ENGINEERING AND DESIGN. - ISSN 0920-3796. - 196:(2023), p. 114023. [10.1016/j.fusengdes.2023.114023]

Availability:

This version is available at: 11583/2982890 since: 2023-10-10T10:26:42Z

Publisher:

Elsevier

Published

DOI:10.1016/j.fusengdes.2023.114023

Terms of use:

This article is made available under terms and conditions as specified in the corresponding bibliographic description in the repository

Publisher copyright

GENERICO preprint/submitted version accettata

This article has been accepted for publication in FUSION ENGINEERING AND DESIGN, published by Elsevier.

(Article begins on next page)

SOLPS-ITER numerical evaluation about the effect of drifts in a divertor configuration of ASDEX-Upgrade and a limiter configuration of J-TEXT

H. Wu¹, P. Shi², F. Subba¹, H. Sun², M. Wischmeier³, R. Zanino¹, the ASDEX Upgrade Team

1.NEMO Group, Dipartimento Energia, Politecnico di Torino, Corso Duca degli Abruzzi 24, 10129 Torino, Italy

2.United Kingdom Atomic Energy Authority, Culham Centre for Fusion Energy, Culham Science Centre, Abingdon, Oxon OX14 3DB, United Kingdom.

3.Max-Planck-Institut für Plasmaphysik, Boltzmannstraße 2, D-85748 Garching, Germany

Abstract:

We performed SOLPS-ITER numerical simulation on the J-TEXT limiter tokamak with the activation of drifts. The simulation results are compared with ASDEX Upgrade divertor simulation results to evaluate the effect of drifts. Through a gas puffing rate scan, both attached and detached regimes were numerically obtained in the AUG divertor and J-TEXT limiter. The key plasma parameters in the J-TEXT limiter are evaluated with and without drifts that have a qualitative performance like AUG except the roll-over of the total ion flux at the targets. The drift effects on the target profiles are investigated for the maximum electron temperature of 15eV and 5eV at the outer targets for both devices. When the outer targets are attached in the J-TEXT limiter and AUG divertor, the drifts result in the partial detachment of the inner targets. In the detached regimes, the drifts decrease the electron temperature on AUG divertor targets. However, for the J-TEXT limiter, the electron temperature only decreases at the far SOL region at the inner target. The effect of drifts on the neutral density is also presented.

1. Introduction

Edge plasma code packages, e.g. SOLPS-ITER[1], UEDGE[2], and SOLEDGE2D[3] are widely used to study boundary plasma behavior in current tokamak devices, e.g. ASDEX Upgrade (AUG)[4] and Alcator C-mod[5], and to explore the potential solution for power exhaust problem of high power scenario of future devices, e.g. DTT [6], SPARC[7] and EU-DEMO[8]. In SOLPS-ITER, two main modules are included: the multi-fluid plasma solver B2.5 [9] for charged species transport in toroidal symmetry, and the Monte Carlo code EIRENE[10], which describes kinetic neutral transport.

The J-TEXT tokamak [11] is a conventional medium-sized tokamak with a major radius of $R_0 = 1.05$ m and minor radius of $a = 0.25\text{--}0.29$ m and the first wall and the limiter are covered with carbon tiles. Recently, similar to the AUG High Field Side High Density (HFSHD) region [4][13][14], a high-density front has been observed in the SOL of J-TEXT [15]. The formation of the HFSHD region is influenced by edge plasma physics, especially the drifts. The physical models of SOLPS-ITER haven't been validated against limiter configuration experimental data. The above reasons motivate us to perform SOLPS-ITER numerical simulations of J-TEXT limiter configuration, which could help in the effort for power exhaust modelling.

In this work, we performed a SOLPS-ITER numerical simulation on the J-TEXT limiter configuration with the activation of full drifts and currents[16][17]. The effect of drifts in the J-TEXT limiter is evaluated through a preliminary comparison with AUG single-null divertor configuration simulation results. In the J-TEXT limiter experimental discharges, there is a lot of carbon impurity that are sputtered from the wall and limiter. However, the carbon impurity is not considered thus we don't aim to reproduce the HFSHD region in this work. The rest of the paper is organized as follows. Section 2 describes the modelling setup. Section 3 compares the effect of drifts in the limiter J-TEXT and divertor AUG, not only in the key parameters,

e.g., upstream density and temperature etc., but also the targets profiles in the attached and detached regimes. The conclusions are the section 4.

2. Modelling setup

The 96×36 quadrilateral mesh for plasma, both for AUG divertor and J-TEXT limiter, and triangular mesh for neutral particle transport are shown in Figure 1. It should be mentioned that there is no Private Flux Region (PRF) in the J-TEXT limiter, and it only contains the core and SOL computational regions. In this study, the point where the LCFS is tangentially in contact with the Limiter targets termed as O-point and is similar to the X-point in divertor configuration.

For the AUG divertor, the gas puffing position is at the outer mid-plane and the pumping and settings are inherited from previous study [4]. For the J-TEXT limiter, the gas puffing location is at the bottom of wall according to experiments[15]. Considering the Carbon material of the first wall in the J-TEXT, a pumping albedo of 0.9 is used at all wall elements to mimic the Carbon absorption. We only considered pure deuterium and hydrogen for AUG divertor and J-TEXT Limiter, respectively. At the core boundary, the ion fluxes are equal to the neutral particle flux across the core boundary, and no other core fueling is considered. Other boundary conditions which are not the same as our previous modelling[4] are summarized in Table 1. This is because we found with these values, current J-TEXT Limiter simulation results are not far away from experimental measurements, which are helpful for our future validation. The default set of EIRENE[18] reactions in SOLPS-ITER is employed which include the Kotov-2008 model[19] and neutral-neutral collision[20].

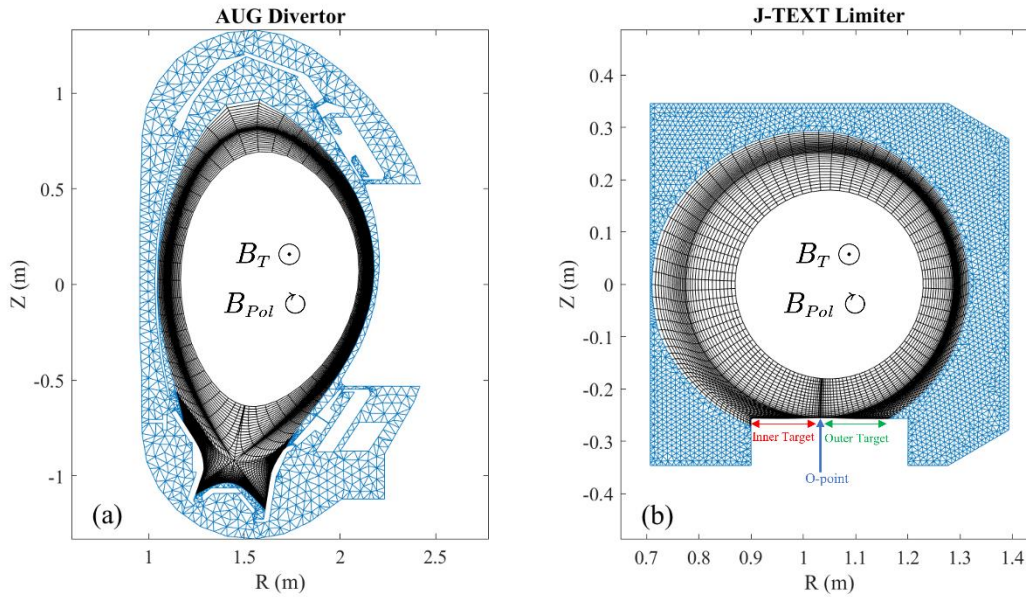


Figure 1 Computational meshes for (a) AUG divertor and (b) J-TEXT limiter.

Table 1 Boundary conditions for the AUG divertor and J-TEXT limiter simulation.

	AUG divertor	J-TEXT limiter
Input Power	0.6MW	0.316MW
Leakage factor for ion density at the north boundary	-0.01	-0.001
Leakage factor for ion temperature at the north boundary	-0.01	-0.001
Leakage factor for ion thermal velocity at the north boundary	-1.0e-4	-1.0e-4

In order to exclude the effect of perpendicular transport, which have a strong impact on simulation results, the constant values of perpendicular transport coefficients are used both in AUG and J-TEXT. Based on the AUG 16151 benchmark cases [20] which are provided in SOLPS-ITER code package, the same level of transport coefficients that $D_{\perp} = 0.5 \text{ m}^2/\text{s}$, $\chi_{\perp,ion} = \chi_{\perp,electron} = 1.6 \text{ m}^2/\text{s}$ were selected instead of adjusting transport coefficients to match experimental upstream profiles. The validated physical models, except the perpendicular transport, from [4][22], are used for both AUG divertor and J-TEXT limiter. The $E \times B$ and diamagnetic drifts and all currents (parallel electric current, anomalous current, diamagnetic current, inertial current, ion-neutral current, current due to perpendicular and parallel viscosity, current due to viscosity tensor) are activated.

3. Results and discussions

3.1 Gas puffing scan

We performed a gas puffing rate scan [23] with and without drifts for both AUG divertor and J-TEXT limiter. The gas puffing rate $\Gamma_{\text{puff},D2}$ is from 1.0×10^{21} D/s to 6.0×10^{21} D/s and from 3.0×10^{20} D/s to 1.2×10^{21} D/s for the AUG divertor and J-TEXT limiter respectively. The performance of key plasma parameters, including outer mid-plane (OMP) electron density $n_{e,omp}$ and OMP temperature $T_{e,OMP}$, maximum electron density at the inner and outer targets $n_{e,IT}$ and $n_{e,OT}$, maximum electron temperature at the inner and outer targets $T_{e,IT}$ and $T_{e,OT}$, the total ion flux at the inner and outer targets $\Gamma_{ion,IT}$ and $\Gamma_{ion,OT}$, are presented in Figure 2. In Figure 2 (a) and (b), it can be found that as gas puffing rate increase, the $n_{e,omp}$ increase and $T_{e,OMP}$ decrease for both with and without drifts in AUG divertor and J-TEXT limiter. When the gas puffing rate is low, the drifts effect is not strong. However, when the gas puffing value is high, the drifts effect on $n_{e,omp}$ is larger and results in the $n_{e,OMP} \sim 15\%$ higher than the non-drift cases. When the gas puffing rate is high, the drifts decrease the maximum density at the inner and outer targets in J-TEXT limiter as shown in Figure 2 (c) and (d). This is because the poloidal drifts move the high density, which is near the O-point and due to the ionization of recycled neutral from targets, to the upstream location. Through gas puffing rate scan with the activation of drifts, the max $T_{e,OT}$ ranges from 16eV to 3eV and 25eV to 4eV in the AUG divertor and J-TEXT limiter, respectively as shown in Figure 2 (e) and (f). From attached regimes to detached regimes [24] are numerically achieved in the AUG divertor and J-TEXT limiter. The differences between with and without drifts are within 20%. In Figure 2 (g) and (h), there is no roll-over of the $\Gamma_{ion,IT}$ and $\Gamma_{ion,OT}$ in the J-TEXT limiter as observed in the AUG divertor. This is because the recycled neutrals from J-TEXT limiter targets directly cross the Last Closed Flux Surface (LCFS) into the core region, then ionize as ions that transport along the closed magnetic field lines. No recombination front [25] is formed in the J-TEXT limiter SOL. Even with a high gas puffing rate and max $T_{e,OT}$ below 5eV for both with and without drifts, there is no rollover of total ion flux in J-TEXT limiter. We believe that in these conditions the J-TEXT limiter is in the detach regime [24]. Compared to the non-drifts cases, in the detached regime

in both AUG divertor and J-TEXT limiter, the drifts result in a lower total ion flux at both the inner and outer targets. In this study, the max $T_{e,OT}$ is selected as an indicator of the detachment of J-TEXT limiter, because there is no roll-over of particle flux at the targets.

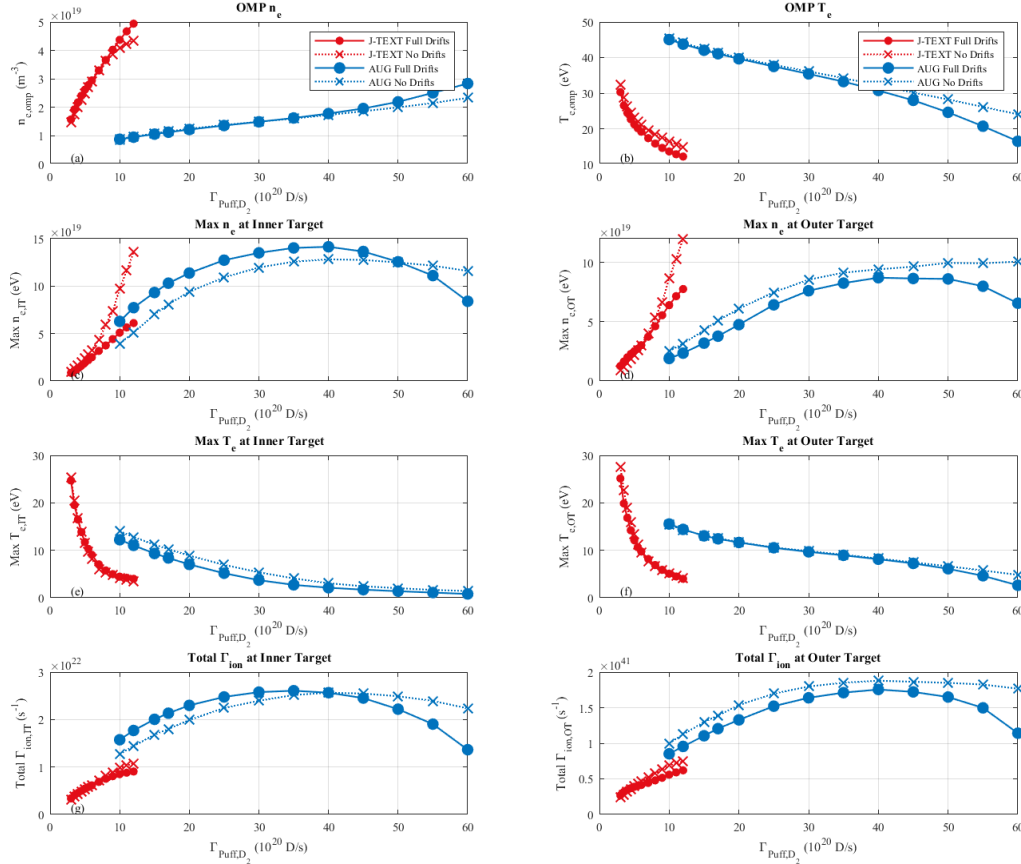


Figure 2 The AUG divertor and J-TEXT limiter key plasma parameters behavior with and without drifts under D_2 gas puffing rate scan, including (a) Electron density at the outer mid-plane $n_{e,OMP}$, (b) Electron temperature at the outer mid-plane $T_{e,OMP}$, (c) Maximum electron density at the inner target, (d) Maximum electron density at the outer target, (e) Maximum electron temperature at the inner target $T_{e,IT}$, (f) Maximum electron temperature at the at the outer target $T_{e,OT}$, (g) Total ion flux at the inner target $\Gamma_{ion,IT}$ and (h) Total ion flux at the inner target $\Gamma_{ion,OT}$.

3.2 Target profiles

In order to evaluate the drifts effect on the targets profiles, for both AUG divertor and J-TEXT limiter, two types of cases are considered as attached and detached cases, wherein the maximum $T_{e,OT}$ (with drifts) are 15eV and 5eV, respectively. The upstream profiles of J-TEXT limiter are shown in Figure 3. For the attached cases, the electron pressure balance [26] and electron temperature at the targets for the AUG divertor and J-TEXT limiter are shown in Figure 4 and 5. The drifts have no impact on the upstream electron pressure but result in the decrease of electron pressure and temperature of the AUG divertor along the inner target. For the J-TEXT limiter, in the high field side, the poloidal drifts, which are strong near the LCFS,

move the particles away from the inner target resulting in a lower pressure in the near SOL region (0-0.5m). In the far SOL region (0.05-0.15m), there is no pressure drop, and the radial drifts result in a higher density. In order to satisfy the pressure balance, there is a lower temperature in the far SOL region at the inner target.

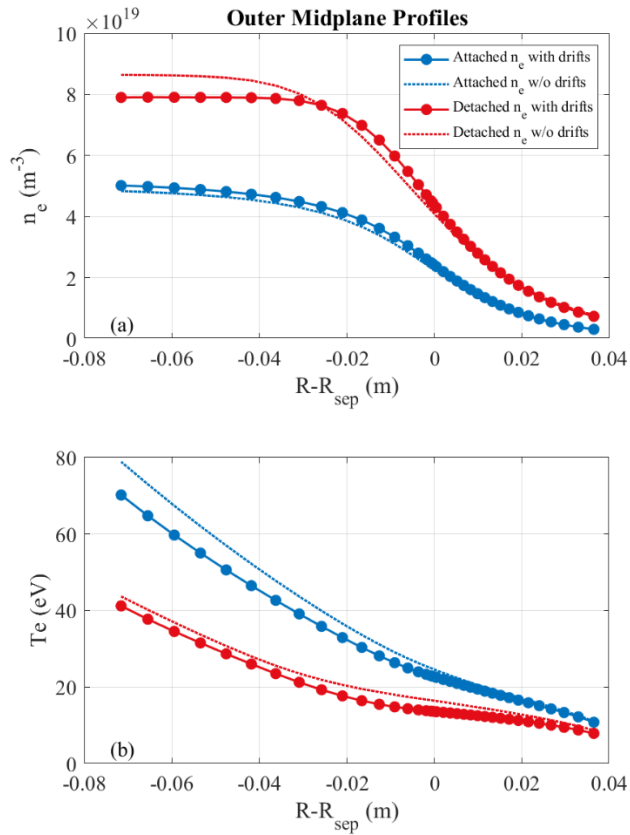


Figure 3 J-TEXT limiter Outer Midplane profiles for (a) electron density and (b) is electron temperature.

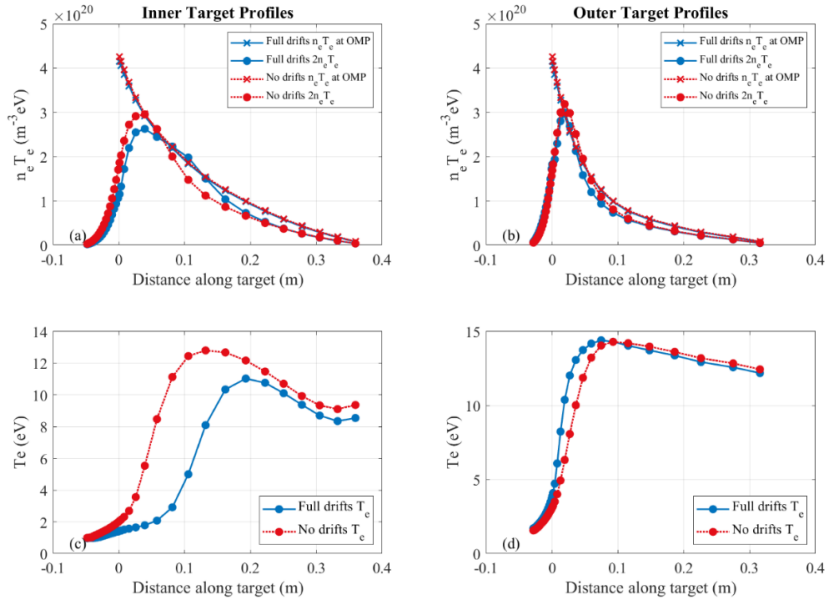


Figure 4 AUG divertor target profiles for the attached cases. (a) is electron pressure balance at the inner target, (b) is electron pressure balance at the outer target, (c) is the electron temperature at the inner target and (d) is the electron temperature at the outer target.

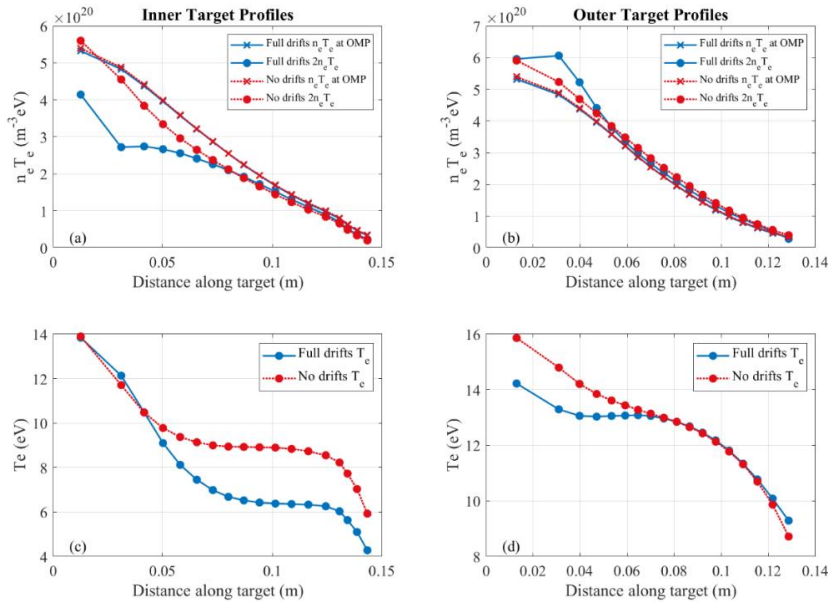


Figure 5 J-TEXT Limiter target profiles for the attached cases. (a) is electron pressure balance at the inner target, (b) is electron pressure balance at the outer target, (c) is the electron temperature at the inner target and (d) is the electron temperature at the outer target.

For the detached cases, the simulation results about target profiles are shown in Figure 6 and 7. Compared with non-drift cases, the drifts result in a lower electron pressure at the upstream and targets both in the AUG divertor and J-TEXT limiter. However, in J-TEXT limiter, the drifts lead to a higher electron temperature of the outer target and the near SOL region of the inner target, which is the opposite of the AUG divertor. For the non-drifts detached case, there is a density front in the core region near the O-point

as shown in Figure 8 (d), which is due to the ionization of recycling neutral from the inner and outer targets. The ionization front, as shown in Figure 9 (d), is an energy sink that leads to a low temperature ($\sim 3\text{eV}$) region near the O point. This explains why in the detached regimes, there is a low temperature ($\sim 3\text{eV}$) in the near SOL region at both inner and outer targets as shown in Figure 7 (c) and (d). With the activation of drifts, the poloidal $E \times B$ drift in the core region is in the counterclockwise direction that transports particles and energy from the high field side to the low field side upstream. The poloidal $E \times B$ drift eliminates the density front, as shown in Figure 8 (c), and compensates that energy sink due to ionization. Thus, the temperature near the O-point increases compared to the non-drift detach case. However, this mechanism does not affect the far SOL region. In the far SOL region, the radial $E \times B$ transport is dominant that decreases the density in the low field side far SOL region, and increases the density in the high field side far SOL region. In order to satisfy the pressure balance, an asymmetry of target temperature profiles in the far SOL region arises. Besides, the length of the cell in the J-JTEXT limiter SOL near the O-point is larger than the others which might lead to a numeric uncertainty.

In Figure 8(c), with the activation of drifts, we don't observe the HFSHD region [12][14] in the J-TEXT Limiter. One possible explanation is there isn't the PFR in the J-TEXT limiter. In divertor configuration, the drifts move particles from the outer divertor region to the PFR and then from the PFR to the inner divertor region. This mechanism is associated with the inner-outer asymmetry of detachment and the formation of the HFSHD. However, in the J-TEXT limiter configuration, there isn't such a mechanism.

In our simulation, the heat flux boundary condition is selected at the core boundary. Thus, the radial electron and ion heat fluxes can be treated as constant values. If there are higher values of the $\chi_{\perp, ion}$ and $\chi_{\perp, electron}$, the gradient of T_e will become smaller and the T_e will increase inside the LCFS near the O-point. Then it will result in a higher value of T_e in the near SOL region of the targets. In the far SOL region, there is no strong pressure drop and the profiles of T_e at the inner and outer targets will be more flat because of the smaller gradient of T_e .

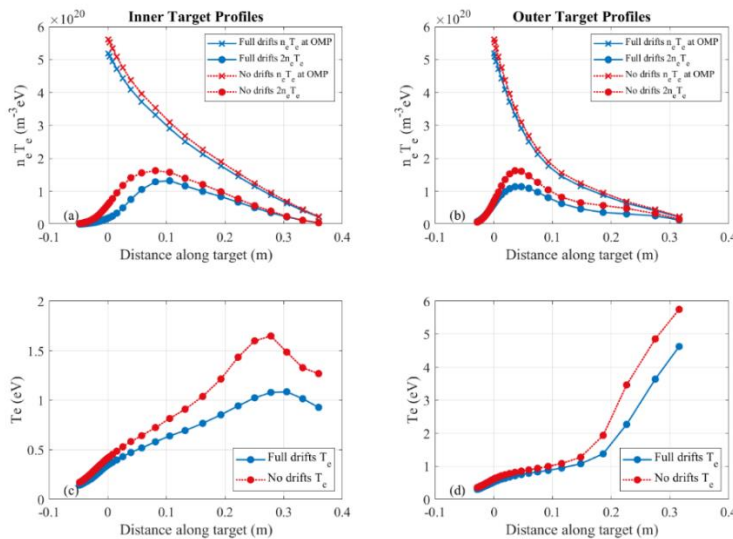


Figure 6 AUG divertor target profiles for the detached cases. (a) is electron pressure balance at the inner target, (b) is electron pressure balance at the outer target, (c) is the electron temperature at the inner target and (d) is the electron temperature at the outer target.

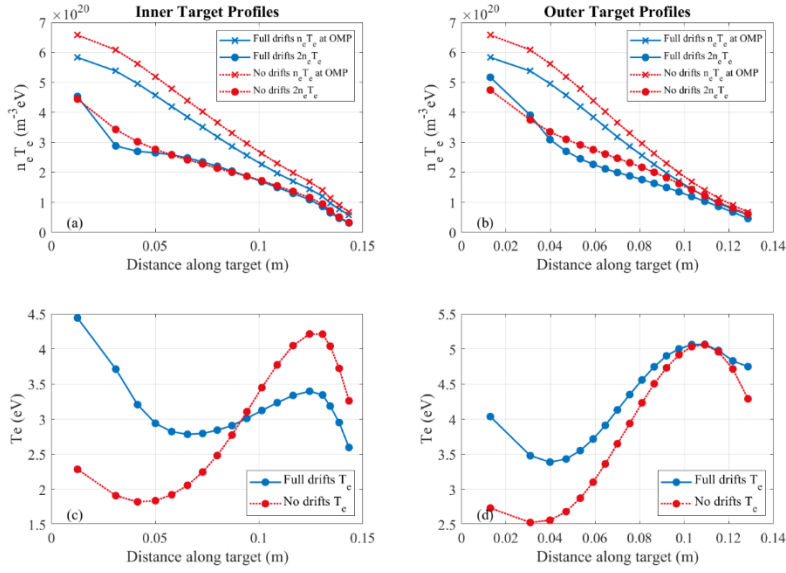


Figure 7 J-TEXT Limiter target profiles for the detached cases. (a) is electron pressure balance at the inner target, (b) is electron pressure balance at the outer target, (c) is the electron temperature at the inner target and (d) is the electron temperature at the outer target

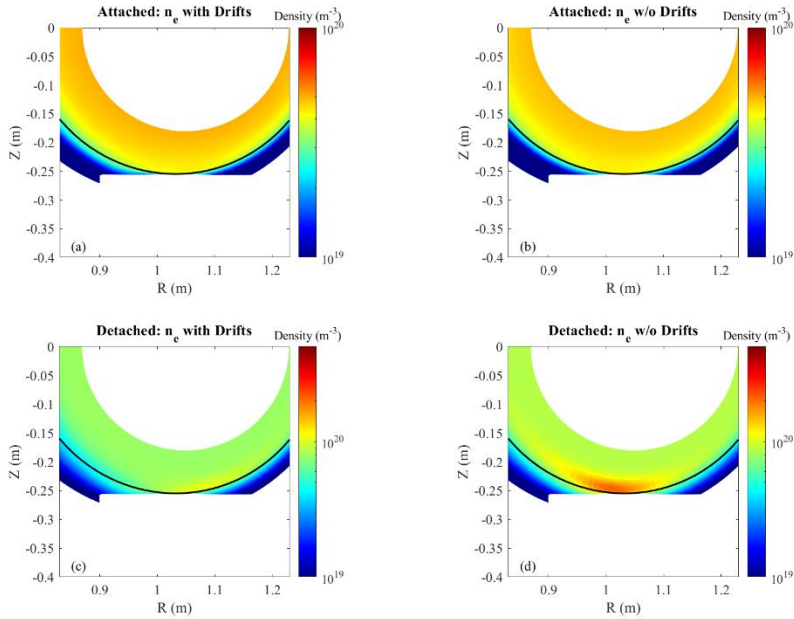


Figure 8 J-TEXT Limiter 2D distribution of electron density n including: (a) attached case with drifts, (b) attached case w/o drifts, (c) detached case with drifts and (d) detached case w/o drifts.

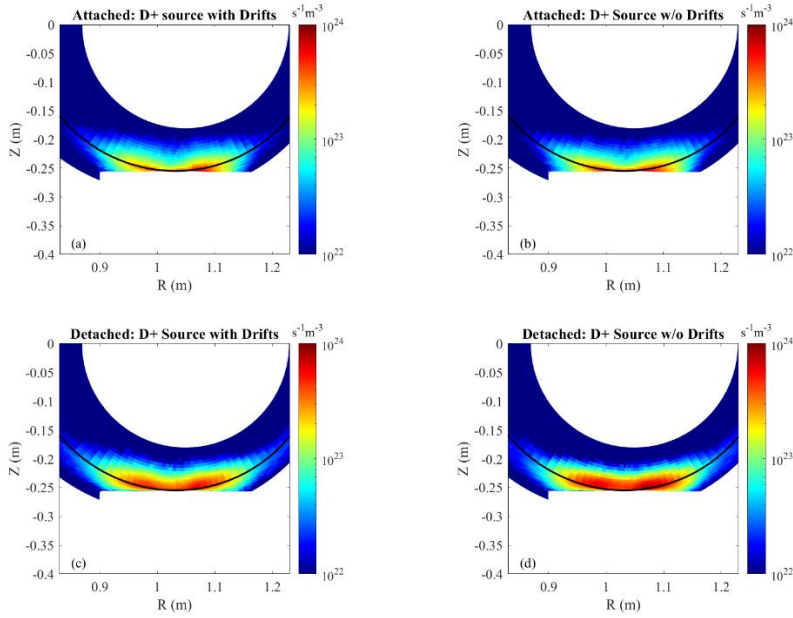


Figure 9 J-TEXT Limiter 2D distribution of D+ source including: (a) attached case with drifts, (b) attached case w/o drifts, (c) detached case with drifts and (d) detached case w/o drifts.

3.3 Neutral density distribution

Figure 10 shows the neutral particle density ($D+2D_2$) distributions in the AUG divertor and J-TEXT limiter for the attached and detached cases with the activation of drifts. The neutral density in SOL region near targets in AUG divertor is \sim two order magnitude higher than the one in J-TEXT limiter. This is consistent with the fact that the roll-over of total ion flux is only observed in AUG divertor due to the strong recombination front. The complicated sub-divertor structures in AUG [4][14], which are not exist in the J-TEXT limiter, may also contributes to the high neutral density. Figure 11 shows the ratio of neutral density between with and without drifts. For the attached cases, the drifts result in a higher neutral density in the high field side of both AUG and J-TEXT, which is consistent that the drifts lead to the inner target partially detached. For the detached cases, in AUG divertor, the drifts result in a higher neutral density in the divertor entrance. This is because the formation of recombination front which is near the divertor entrance. However, for the J-TEXT limiter, the drifts lead to a lower neutral density near the O-point in the core region and SOL region in the detached case. This is because the drifts, on the one hand, reduce the electron density, on the other hand, increase the temperature as mentioned in section 3.2, which leads to the lower formation of neutral particles due to recombination. In the future, we will investigate in detail how the $E \times B$ drifts and diamagnetic drifts separately affect the particle flux and temperature.

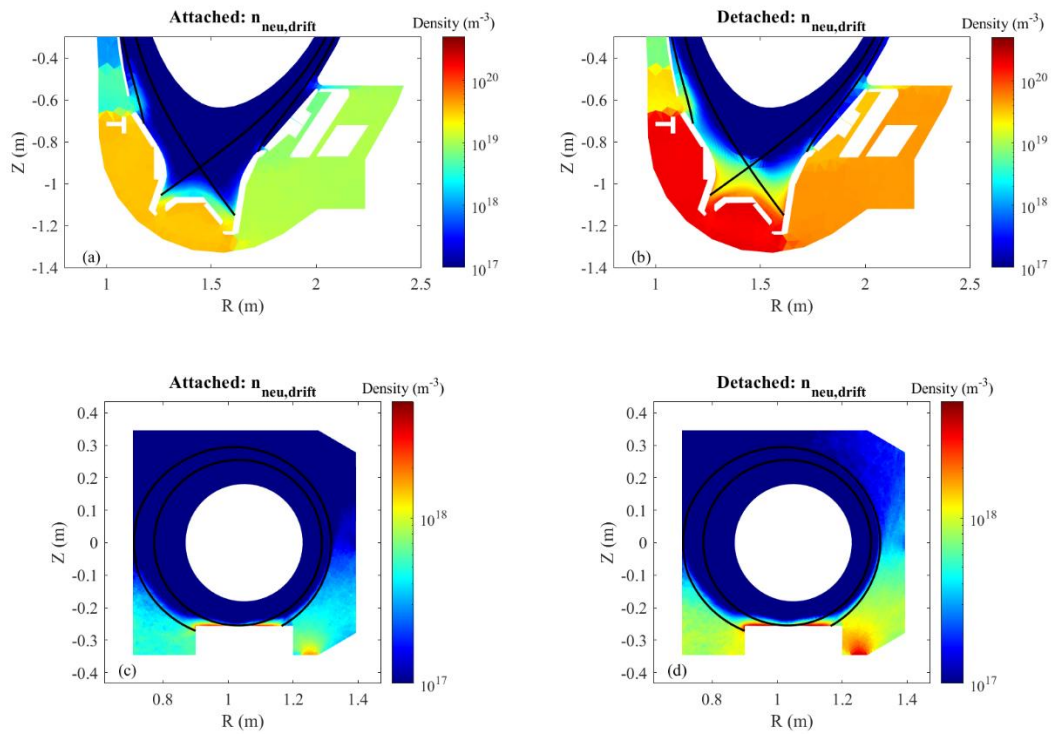


Figure 10 Neutral density ($D+2D_2$) distributions with the activation of drifts. (a) is AUG divertor in attached case, (b) is AUG divertor in detached case, (c) is J-TEXT limiter in attached case and (d) is (c) J-TEXT limiter in detached case.

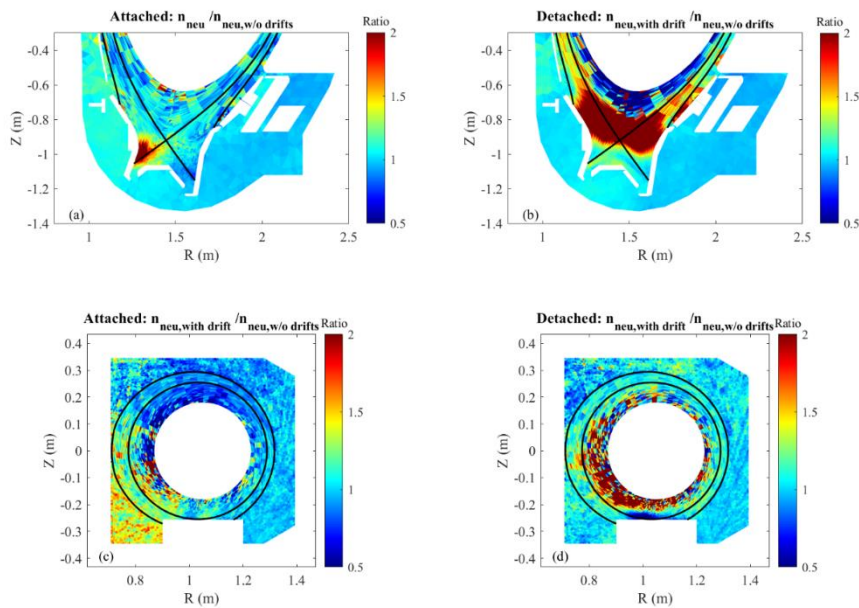


Figure 11 The ratio of neutral density ($D+2D_2$) between with and without drift. (a) is AUG divertor in attached case, (b) is AUG divertor in detached case, (c) is J-TEXT limiter in attached case and (d) is (c) J-TEXT limiter in detached case.

4. Conclusions

In this work, SOLPS-ITER numerical simulations on the J-TEXT limiter configuration are performed with and without the activation of drifts. The simulation results are compared with ASDEX upgrade results to assess the effect of drifts. The gas puffing rate scan show that all the key plasma parameters except the total ion flux in the J-TEXT limiter have a qualitatively similar performance to the AUG divertor simulation results. The recycled neutrals from limiter targets comes directly into the core region and there is no recombination front in the limiter SOL. Attached and detached cases are selected, in which the maximum $T_{e,OT}$ are 15eV and 5eV respectively, to evaluate the effect of drifts on the target profiles. In the attached cases, the drifts result in the partial detachment of inner target both in the AUG divertor and J-TEXT limiter. For the detached cases, the drifts decrease electron temperature in the AUG divertor targets but increase the electron temperature near the O-point at the J-TEXT limiter targets. This is because the poloidal drifts move the ions generated from the ionization of recycled neutrals to the upstream location and also transport energy to the vicinity of the O-point. The effect of drifts on neutral density distribution is also discussed. The drifts lead to a higher neutral density in the attached cases in both the AUG divertor and the J-TEXT limiter. In the detached cases, the drifts lead to a lower neutral density near the O-point of J-TEXT which is opposite to AUG.

In the future, the J-TEXT limiter simulation results will be validated against experimental data by adjusting the transport coefficients. Carbon impurity and different limiter positions will also be considered.

Acknowledgements

The authors would like to thank Dr.X. Bonnin for his useful discussions about the neutral particle transport in limiter. This work has been carried out within the framework of the EUROfusion Consortium, funded by the European Union via the Euratom Research and Training Programme (Grant Agreement No 101052200 — EUROfusion). Views and opinions expressed are however those of the author(s) only and do not necessarily reflect those of the European Union or the European Commission. Neither the European Union nor the European Commission can be held responsible for them. This work has been part-funded by the EPSRC Energy Programme (Grant No. EP/W006839/1).

References

- [1] S. Wiesen, et al., The new SOLPS-ITER code package, *Journal of nuclear materials* 463 (2015): 480-484.
- [2] T.D. Rognien et al., A fully implicit, time dependent 2D fluid code for modeling tokamak edge plasmas *Journal of nuclear materials*. 196(1992) 347–351
- [3] H. Bufferand et al., Implementation of drift velocities and currents in SOLEDGE2D-EIRENE, *Nucl. Mater. Energy* 12 (2017) 852–857

- [4] H.Wu et al., SOLPS-ITER modeling of ASDEX Upgrade L-mode detachment states, *Plasma Physics and Controlled Fusion* 63.10 (2021): 105005.
- [5] W. Dekeyser et al., SOLPS-ITER modeling of the Alcator C-Mod divertor plasma, *Plasma and Fusion Research* 11 (2016): 1403103-1403103.
- [6] M. Moscheni et al., Cross-code comparison of the edge codes SOLPS-ITER, SOLEDGE2D and UEDGE in modelling a low-power scenario in the DTT, *Nuclear Fusion* 62.5 (2022): 056009.
- [7] S. B. Ballinger et al., Simulation of the SPARC plasma boundary with the UEDGE code, *Nuclear Fusion* 61.8 (2021): 086014.
- [8] F. Subba et al., SOLPS-ITER modeling of divertor scenarios for EU-DEMO, *Nuclear Fusion* 61.10 (2021): 106013.
- [9] B.J. Braams, A multi-fluid code for simulation of the edge plasma in tokamaks, Next European Torus Report (1987) EUR-FU/XII-80/87/68.
- [10] D. Reiter et al., The EIRENE and B2-EIRENE codes, *Fusion Science Technology* 47.2 (2015): 172–186.
- [11] Liang, Y., et al. "Overview of the recent experimental research on the J-TEXT tokamak." *Nuclear Fusion* 59.11 (2019): 112016.
- [12] S. Potzel et al., A new experimental classification of divertor detachment in ASDEX Upgrade, *Nucl. Fusion* 54(2015):013001.
- [13] L. Aho-Mantila, et al., Assessment of SOLPS5. 0 divertor solutions with drifts and currents against L-mode experiments in ASDEX Upgrade and JET, *Plasma Physics and Controlled Fusion* 59.3 (2017): 035003.
- [14] F. Reimold, et al., The high field side high density region in SOLPS-modeling of nitrogen-seeded H-modes in ASDEX Upgrade, *Nuclear Materials and Energy* 12 (2017): 193-199.
- [15] P. Shi et al., Observation of the high-density front at the high-field-side in the J-TEXT tokamak, *Plasma Physics and Controlled Fusion* 63.12 (2021): 125010.
- [16] V. Rozhansky et al., New B2SOLPS5. 2 transport code for H-mode regimes in tokamaks, *Nuclear fusion* 49.2 (2009): 025007.
- [17] E. Kaveeva, et al., Speed-up of SOLPS-ITER code for tokamak edge modeling, *Nuclear Fusion* 58.12 (2018): 126018.
- [18] D. Reiter, The EIRENE code user manual, 2019. <https://www.eirene.de/Documentation/eirene.pdf>
- [19] V. Kotov, et al., Numerical modelling of high density JET divertor plasma with the SOLPS4. 2 (B2-EIRENE) code, *Plasma physics and controlled fusion* 50.10 (2008): 105012
- [20] V. Kotov, Numerical study of the ITER divertor plasma with the B2-EIRENE code package, Forschungszentrum Juelich (Germany). Inst. fuer Energieforschung (IEF), 2007.
- [21] X. Bonnin et al., Full-tungsten plasma edge simulations with SOLPS, *Journal of nuclear materials* 415.1 (2011): S488-S491.
- [22] H. Wu et al., Comparison of SOLPS5. 0 and SOLPS-ITER simulations for ASDEX upgrade L-mode, *Contributions to Plasma Physics* 60.4 (2020): e201900120.
- [23] D. P. Coster, Detachment physics in SOLPS simulations, *Journal of nuclear materials* 415.1 (2011): S545-S548.

- [24] G.F. Matthews, Plasma detachment from divertor targets and limiters, *Journal of nuclear materials* 220 (1995): s104-116.
- [25] F. Reimold, Experimental studies and modeling of divertor plasma detachment in H-mode discharges in the ASDEX upgrade tokamak. Ph.D thesis, **2015**.
- [26] B. Lipschultz, et al., Divertor physics research on Alcator C-Mod, *Fusion science and technology* 51.3 (2007): 369-389.